

SUPPORTING INFORMATION

Carboxylated Wood Membranes for Selective Capture and Recovery of Critical and Commodity Metal Cations

Antoni Sánchez-Ferrer^{1,*}, Devika Upadhye¹, Muzamil Jalil Ahmed^{1,2,*}, Baohu Wu³

¹ Wood Materials Science, Wood Research Institute of Munich (HFM), Technical University of Munich, Winzererstrasse 45, 80797 Munich, Germany

² School of Life Sciences, Technical University of Munich, Maximus von Imhof Forum 2, 85354 Freising, Germany

³ Jülich Centre for Neutron Science (JCNS) at Heinz Maier-Leibnitz Zentrum (MLZ), Forschungszentrum Jülich, 85748 Garching, Germany

* Corresponding Authors: Antoni Sánchez-Ferrer and Muzamil Jalil Ahmed

ORCID: orcid.org/0000-0002-1041-0324

Email: sanchez.ferrer@tum.de

ORCID: orcid.org/0000-0003-1989-9303

Email: muzamil.jalil@tum.de

Fig. SI-1. UV-Vis spectra of the Li ⁺ permeate solutions	page 2
Fig. SI-2. UV-Vis spectra of the Fe ³⁺ permeate solutions	page 3
Fig. SI-3. Li ⁺ and Fe ³⁺ filtration performance across cycles	page 4
Fig. SI-4. UV-Vis spectra of the Li ⁺ standard solutions	page 5
Fig. SI-5. UV-Vis Li ⁺ calibration curve	page 6
Fig. SI-6. UV-Vis spectra of the Fe ³⁺ standard solutions	page 7
Fig. SI-7. UV-Vis Fe ³⁺ calibration curve	page 8

Table SI-1. Li ⁺ filtration efficiency for the SSp and MSp membranes (three cycles)	page 9
Table SI-2. Fe ³⁺ filtration efficiency for the SSp and MSp membranes (three cycles)	page 9
Table SI-3. Cycle-wise filtration efficiency loss for the SSp and MSp membranes	page 9
Table SI-4. Li ⁺ and Fe ³⁺ filtration flux values for the SSp and MSp membranes	page 10
Table SI-5. Theoretical ion-exchange capacity and derived maximum uptake capacities	page 10

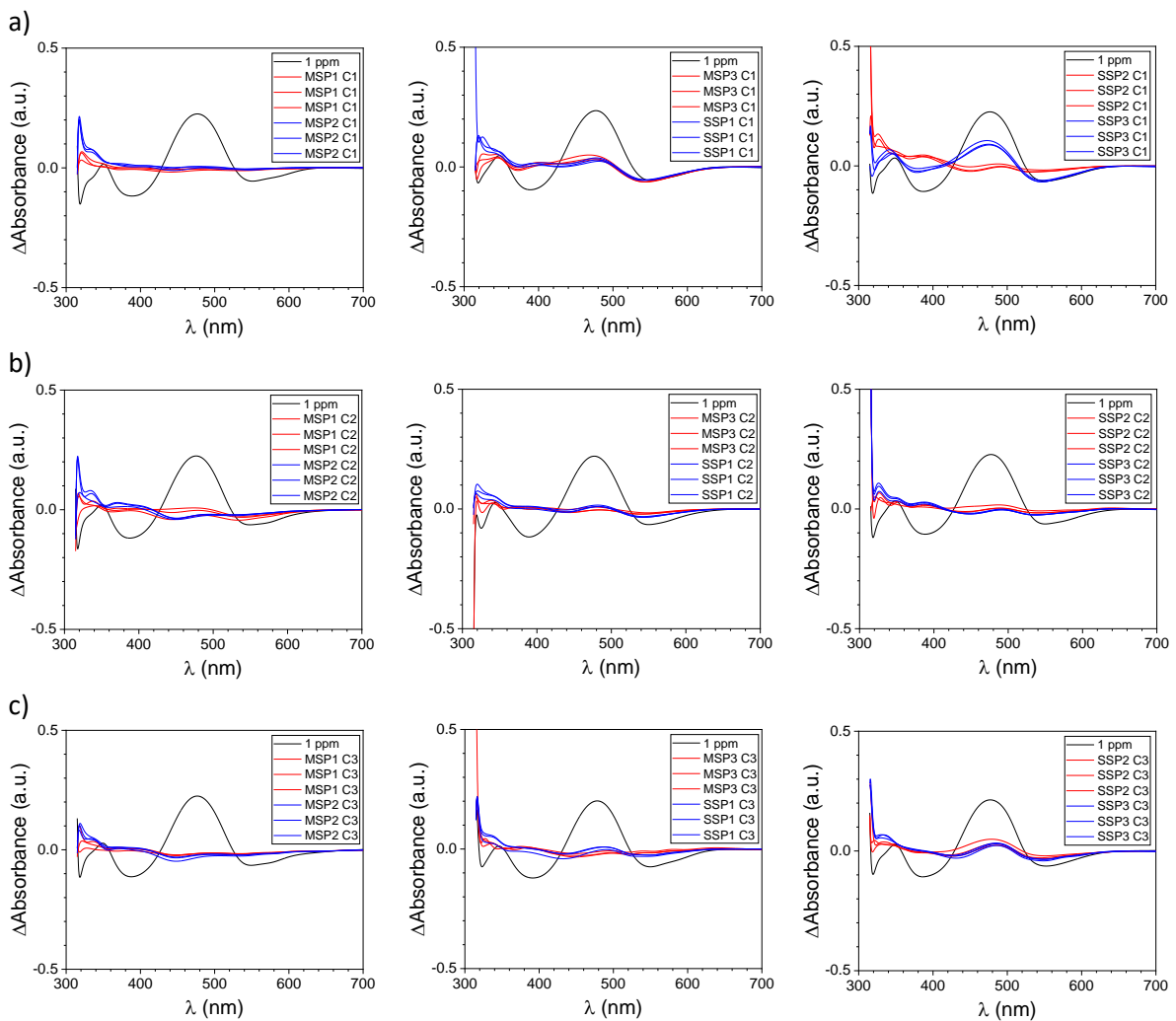


Fig. SI-1. UV-Vis spectra after subtracting the spectra of the 0 ppm Li^+ solution to determine the Li^+ concentration after filtration of a 1 ppm Li^+ solution using the three SSp and the three MSp wood membranes. The results indicate a decrease in absorbance after the a) first, b) second, and c) third filtration cycle. Each plot shows the triplicate for two modified Sp wood membranes together with the 1 ppm (black) Li^+ solution.

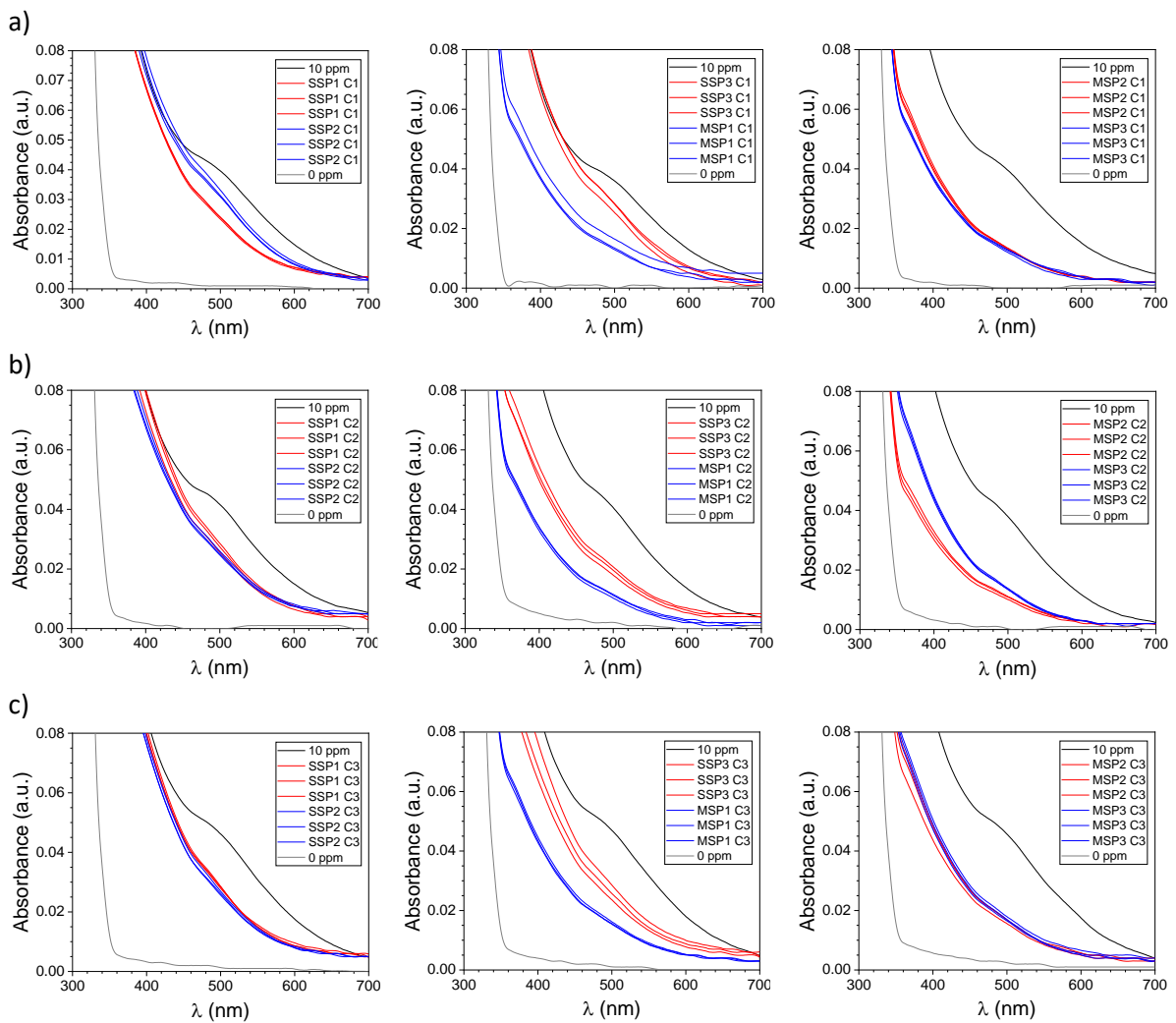


Fig. SI-2. UV-Vis spectra to determine the Fe^{3+} concentration after filtration of a 10 ppm Fe^{3+} solution using the three SSp and the three MSp wood membranes. The results indicate the absorbance decrease after the a) first, b) second, and c) third filtration cycle. Each plot shows the triplicate for two modified Sp wood membranes together with the 10 ppm (black) and the 0 ppm (grey) Fe^{3+} solution.

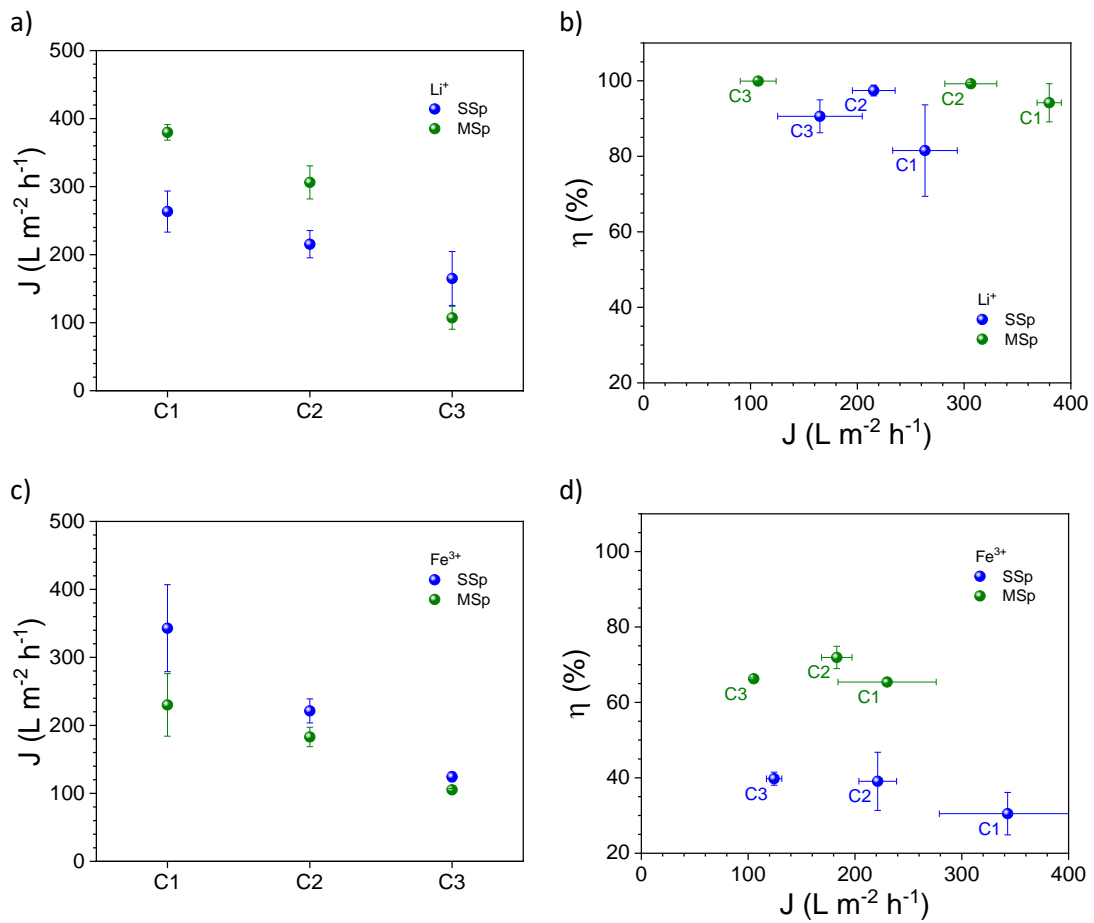


Fig. SI-3. Li⁺ and Fe³⁺ filtration performance of SSp and MSp membranes across cycles. Average filtration fluxes J for a) 1 ppm Li⁺ and b) 10 ppm Fe³⁺ solutions, using the three SSp and the three MSp wood membranes. Cycle-wise average filtration efficiency values η versus average filtration fluxes J for c) 1 ppm Li⁺ and d) 10 ppm Fe³⁺ solutions, using the three SSp and the three MSp wood membranes.

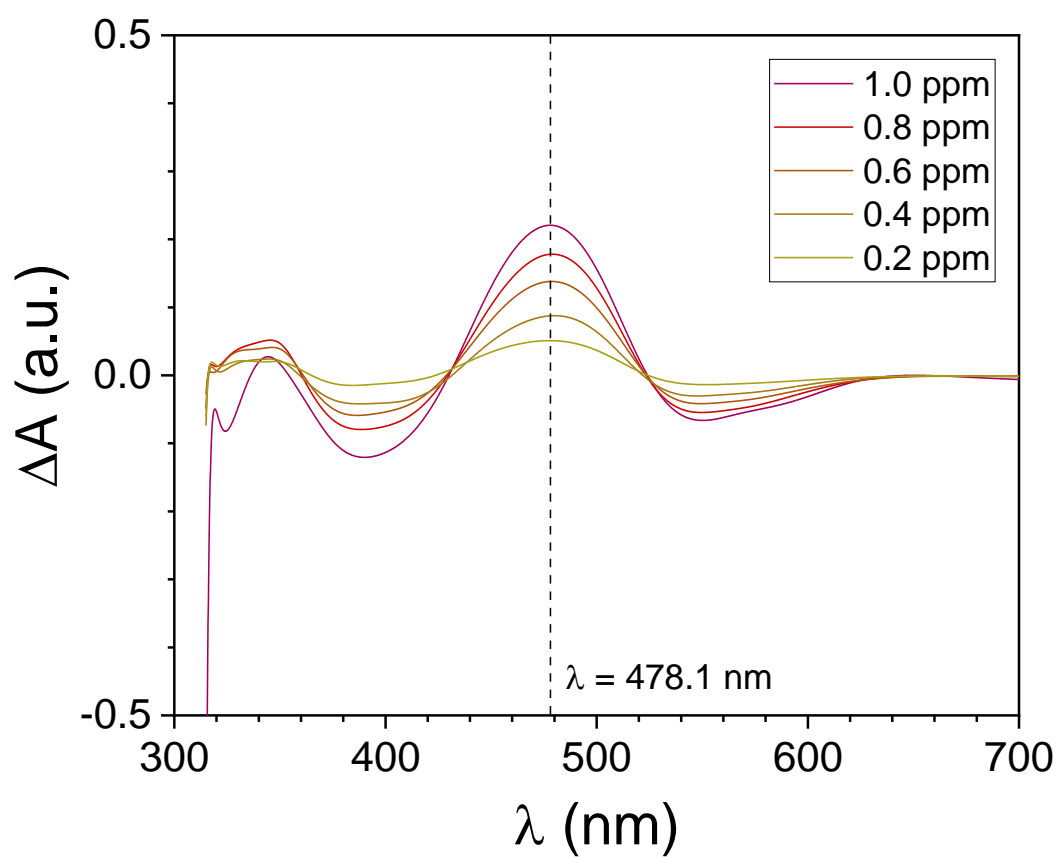


Fig. SI-4. UV-Vis spectra of the Li⁺ solutions at different concentrations from 0.2 ppm to 1.0 ppm obtained after subtracting the 0 ppm Li⁺ solution.

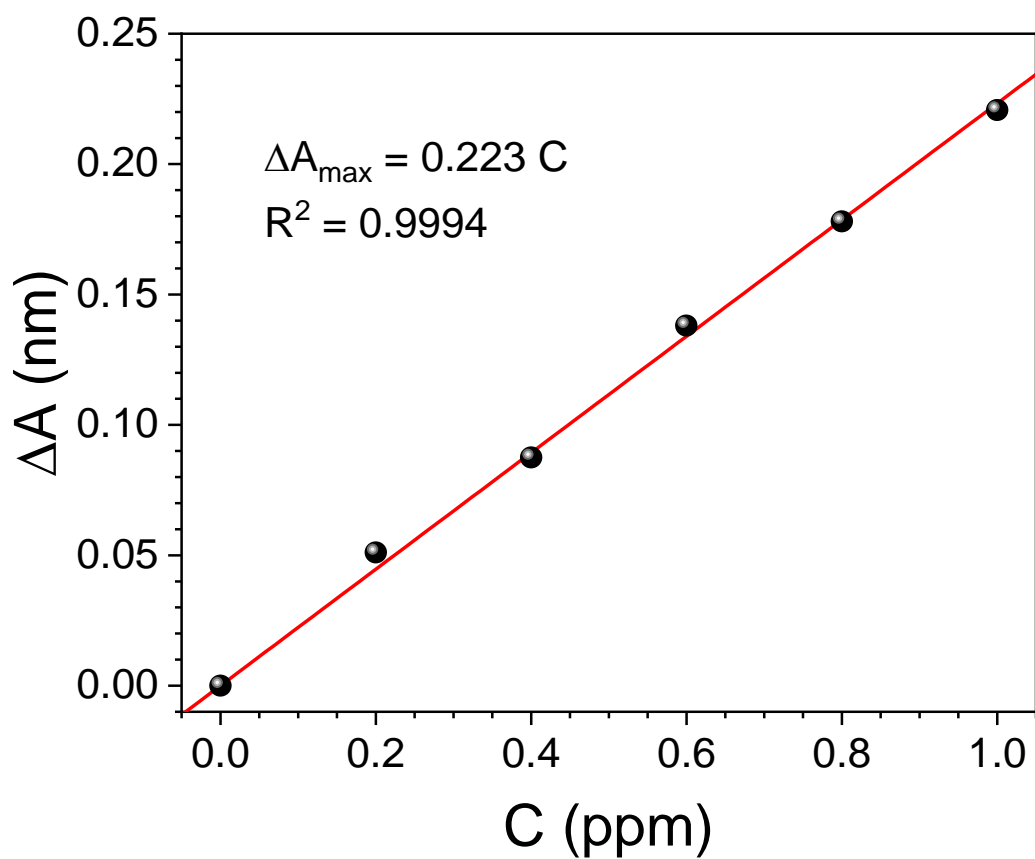


Fig. SI-5. Li^+ calibration curves obtained from the absorbance difference of the peak maxima ΔA_{\max} at 478.1 nm after subtracting the spectra of the 0 ppm Li^+ solution.

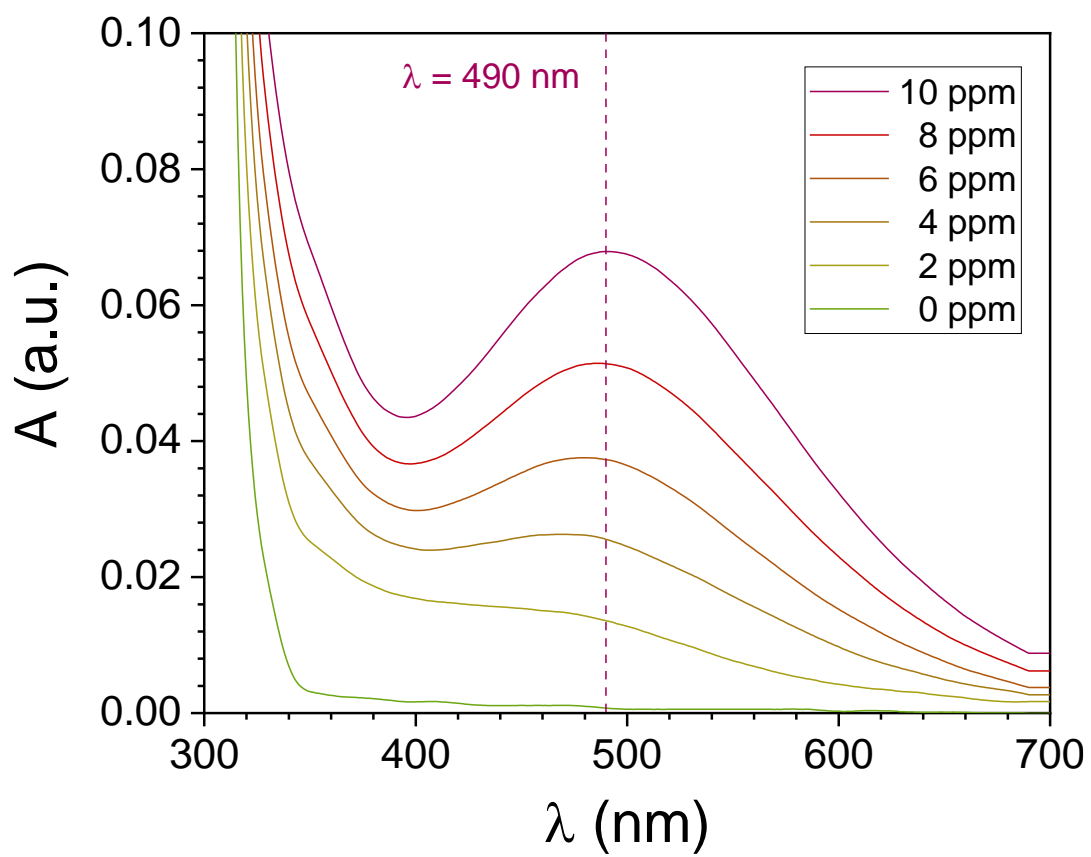


Fig. SI-6. UV-Vis spectra of the Fe³⁺ solutions at different concentrations from 2 ppm to 10 ppm.

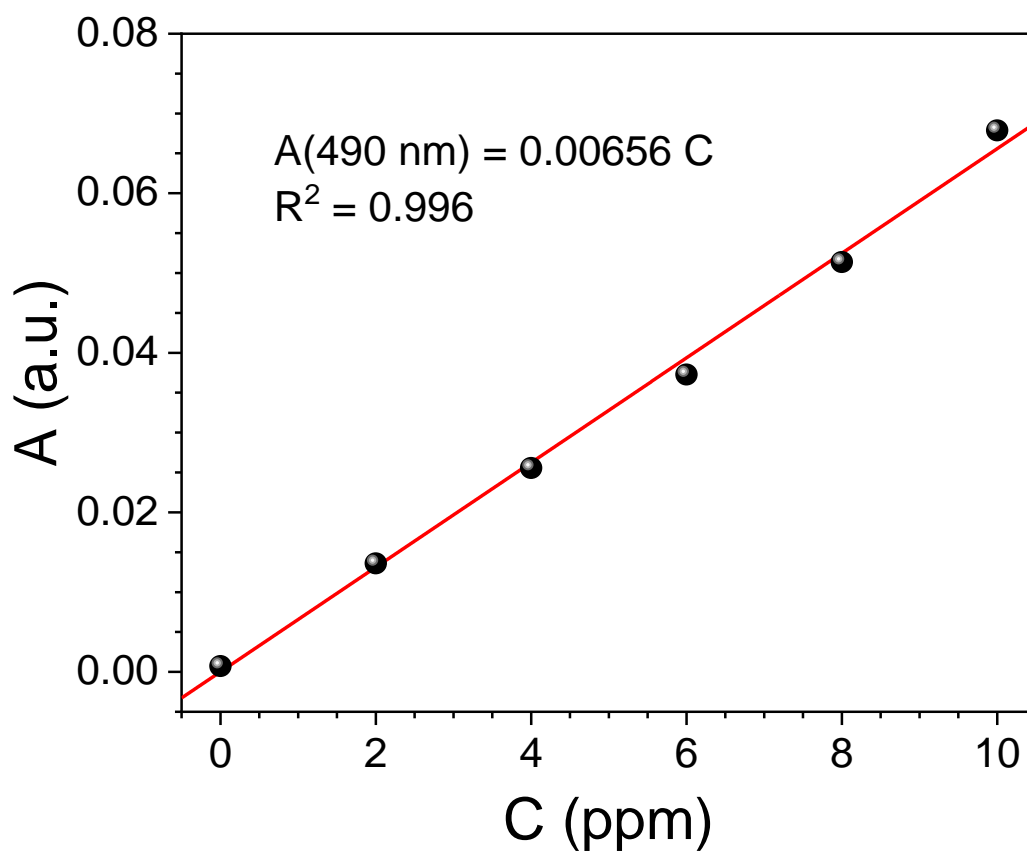


Fig. SI-7. Fe^{3+} calibration curves obtained from the absorbance of the peak maxima A_{max} at 490 nm.

Table SI-1: Li⁺ filtration efficiency values η for the three SSp and the three MSp wood membranes during the three filtration cycles obtained from the analysis of the absorbance difference of the peak maximum ΔA_{\max} at 478 nm after subtracting the spectra of the 0 ppm Li⁺ solution.

ΔA (478 nm) samples	η (%)		
	C1	C2	C3
SSp1	87.1 ± 1.8	94.9 ± 1.0	99.1 ± 0.9
SSp2	99.1 ± 0.9	97.4 ± 2.2	84.6 ± 3.9
SSp3	58.3 ± 2.4	99.9 ± 0.1	88.1 ± 1.5
MSp1	99.9 ± 0.1	98.9 ± 1.1	99.9 ± 0.1
MSp2	98.5 ± 0.8	99.9 ± 0.1	99.9 ± 0.1
MSp3	84.1 ± 2.2	98.8 ± 1.2	99.9 ± 0.1

Table SI-2. Fe³⁺ filtration efficiency values η for the three SSp and the three MSp wood membranes during the three filtration cycles obtained from the analysis of the absorbance of the peak maxima A_{\max} at 490 nm.

A (490 nm) samples	η (%)		
	C1	C2	C3
SSp1	40.3 ± 0.5	28.8 ± 2.1	36.3 ± 0.6
SSp2	20.8 ± 1.8	34.2 ± 1.0	41.1 ± 1.0
SSp3	30.5 ± 2.4	54.2 ± 2.0	41.9 ± 3.4
MSp1	64.2 ± 2.6	75.6 ± 0.9	66.0 ± 0.6
MSp2	64.9 ± 0.2	74.1 ± 0.8	67.2 ± 1.1
MSp3	67.1 ± 0.6	66.1 ± 0.4	65.6 ± 1.1

Table SI-3. Cycle-wise filtration efficiency loss η_{n+1}/η_1 for Li⁺ and Fe³⁺ for the three SSp and the three MSp wood membranes.

samples	Li ⁺		Fe ³⁺	
	η_2/η_1	η_3/η_1	η_2/η_1	η_3/η_1
SSp1	1.09 ± 0.04	1.14 ± 0.04	0.72 ± 0.05	0.90 ± 0.02
SSp2	0.98 ± 0.04	0.85 ± 0.07	1.65 ± 0.15	1.98 ± 0.18
SSp3	1.71 ± 0.12	1.51 ± 0.12	1.78 ± 0.15	1.37 ± 0.16
MSp1	0.99 ± 0.04	1.00 ± 0.00	1.18 ± 0.05	1.03 ± 0.04
MSp2	1.01 ± 0.04	1.01 ± 0.01	1.14 ± 0.01	1.04 ± 0.02
MSp3	1.17 ± 0.08	1.19 ± 0.05	0.98 ± 0.01	0.98 ± 0.02

Table SI-4. Li^+ and Fe^{3+} filtration flux values J for the three SSp and the three MSp wood membranes during the three filtration cycles. Membrane area: 1963.5 mm^2 , at room temperature and under gravity.

samples	$\text{Li}^+ - J (\text{L}\cdot\text{m}^{-2}\cdot\text{h}^{-1})$			$\text{Fe}^{3+} - J (\text{L}\cdot\text{m}^{-2}\cdot\text{h}^{-1})$		
	C1	C2	C3	C1	C2	C3
SSp1	213	253	196	392	235	123
SSp2	260	209	213	421	243	137
SSp3	318	185	86	216	186	112
avg	263	215	165	343	221	124
error	30	20	40	64	18	7
MSp1	390	349	139	232	189	102
MSp2	357	265	82	309	204	109
MSp3	392	305	100	150	156	105
avg	380	306	107	230	183	105
error	11	24	17	46	14	2

Table SI-5. Theoretical ion-exchange capacity IEC_{max} and derived maximum uptake capacities q_{max} , from the weight gain w_g .

samples	Basis	w_g (%)	IEC_{max} ($\text{mmol}\cdot\text{g}^{-1}$)	$q_{\text{max}} (\text{Li}^+)$ ($\text{mg}\cdot\text{g}^{-1}$)	$q_{\text{max}} (\text{Fe}^{3+})$ ($\text{mg}\cdot\text{g}^{-1}$)
SSp	COOH-based	36.8	2.69	18.7	50.1
	COONa-based	45.1	2.54	17.6	47.3
MSp	COOH-based	25.1	2.05	14.2	38.1
	COONa-based	30.7	1.96	13.6	36.4